Random-walk model of cotransport

Yan B. Barreto,[1] Béla Suki,[2] and Adriano M. Alencar[1]
[1]*Instituto de Física, Universidade de São Paulo, 05508-090 São Paulo, São Paulo, Brazil*
[2]*Department of Biomedical Engineering, Boston University, Boston, Massachusetts 02215, USA*

(Received 19 December 2019; accepted 15 July 2020; published 10 August 2020)

We present a statistical mechanical model to describe the dynamics of an arbitrary cotransport system. Our starting point was the alternating access mechanism, which suggests the existence of six states for the cotransport cycle. Then we determined the 14 transition probabilities between these states, including a leak pathway, and used them to write a set of Master Equations for describing the time evolution of the system. The agreement between the asymptotic behavior of this set of equations and the result obtained from thermodynamics is a confirmation that leakage is compatible with the static head equilibrium condition and that our model has captured the essential physics of cotransport. In addition, the model correctly reproduced the transport dynamics found in the literature.

DOI: 10.1103/PhysRevE.102.022403

I. INTRODUCTION

Cotransporters are transmembrane carrier proteins that couple the facilitated diffusion of ν_A particles of species A across a biological membrane to the active transport of ν_B particles of species B. Under certain experimental conditions, these proteins can also work in reverse, utilizing the free energy stored in the electrochemical gradient $\Delta\tilde{\mu}_B$ to drive the transport of particles A against the gradient $\Delta\tilde{\mu}_A$ [1]. Cotransporters are divided into symporters and antiporters. In a symport mechanism, the transport direction is the same for both particles A and B, such as in the case of the lactose permease, LacY, which simultaneously transports an H^+ and a lactose across the cell membrane of *Escherichia coli* [2,3]. In contrast, an antiport mechanism, such as the countertransport of Na^+ and Ca^{2+} via the sodium-calcium exchanger, NCX, moves three Na^+ ions into the cell in exchange for one Ca^{2+} transported out of the cell [4].

One of the currently accepted explanations for the cotransport mechanism was proposed more than 50 years ago by Jardetzky in the alternating access model [5]. This model for a symporter with stoichiometry $\nu_B : \nu_A$ is presented in Fig. 1(a). The transport starts with the binding of ν_A particles A from the periplasm to the protein in the outward-facing conformation, C_{Out} (State 1 $\rightarrow$ State 2). Then the binding of ν_B particles B from the the periplasm (2 $\rightarrow$ 3) induces a conformational change to the inward-facing conformation, C_{In} (3 $\rightarrow$ 4). After that, the ν_B particles B are released into the cytoplasm (4 $\rightarrow$ 5), followed by the ν_A particles A (5 $\rightarrow$ 6), and a conformational change to the C_{Out} conformation (6 $\rightarrow$ 1), ending the transport cycle. This symport mechanism corresponds to the transport of particles B in the influx direction, clockwise. However, transport in the opposite direction, counterclockwise, can also be explained by this mechanism, since influx and efflux are functionally symmetric processes [6]. The transport cycle of an antiporter is described in the caption of Fig. 1(b).

The conventional alternating access model presented above assumes that cotransport is a perfectly energy-efficient process with a fixed stoichiometry. However, it was experimentally observed that uncoupled transport can also occur during this conventional stoichiometric process [7]. This uniport-like phenomenon is referred to as "leakage" and is defined as any movement of the driven or driving species down its electrochemical gradient without the intervention of the cotransporter itself [8]. For instance, the symport of Na^+ and glucose via the sodium-glucose cotransporter 1, SGLT1, includes a Na^+ leak current that represents 5%–10% of the maximal cotransport current [9]. One possibility to explain these experimental observations is to modify the conventional Jardetzky model by allowing transitions between states 2 and 5, as shown in Fig. 1. Other possibilities have been studied in Ref. [10].

Although this modified model can theoretically explain both the coupled and uncoupled transport, it has been criticized from a thermodynamic point of view because, according to some authors, it does not converge to the static head equilibrium state [11–14], and thus a full understanding of cotransport is still lacking. In this work, we propose a statistical mechanical model based on the modified alternating access mechanism that we show to be compatible with static head, offering a semianalytical approach to describe the dynamics of any cotransport system.

II. RANDOM-WALK MODEL

We consider a closed system consisting of a cytoplasm and a periplasm with volumes V_c and V_p, respectively, separated by a biological membrane with a constant membrane potential $\Delta\Psi$ across it. Embedded in this membrane, there are n identical and independent cotransporters that can be either symporters or antiporters, but not both. At a given time t, $N_c^S(t)$ and $N_p^S(t)$ particles of species $S \in \{A, B\}$ are in the cytoplasm and periplasm, respectively. In addition, we assume that there are $n_k(t)$ cotransporters in state $k \in \{1, 2, \ldots, 6\}$, such that $\sum_k n_k = n$. As our system is closed, the total number of particles A, N_A, and the total number of particles B, N_B, must be conserved,

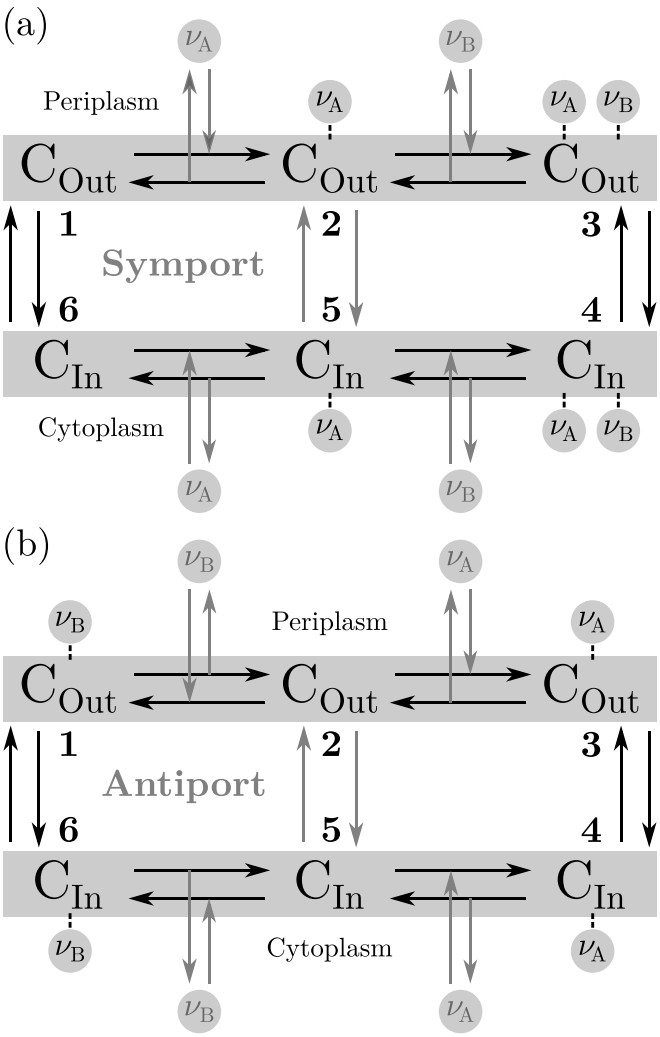

FIG. 1. The alternating access model modified with a leakage pathway between states 2 and 5. (a) The transport cycle of the symport is described in the text. (b) The transport cycle of the antiport starts with the release of ν_B particles B from the protein in the C_{Out} conformation to the periplasm ($1 \rightarrow 2$). Then, the binding of ν_A particles A ($2 \rightarrow 3$) induces a conformational change to the C_{In} conformation ($3 \rightarrow 4$). After that, the ν_A particles A are released into the cytoplasm ($4 \rightarrow 5$), followed by the binding of ν_B particles B ($5 \rightarrow 6$), and a conformational change to the C_{Out} conformation ($6 \rightarrow 1$), ending the transport cycle.

that is,

$$N_A - N_c^A - N_p^A = \nu_A[n_3 + n_4 + (n_2 + n_5)f], \quad (1)$$

and

$$N_B - N_c^B - N_p^B = \nu_B[(n_3 + n_4)f + (1 - f)(n_1 + n_6)], \quad (2)$$

where f is a function whose value is 1 if the proteins are symporters, and 0 if they are antiporters. Note that $N_S - N_c^S - N_p^S$ is the number of S-type particles bound to the cotransporters. The total energy available to do work in this system is given by the change in the Gibbs free energy across the membrane as

$$\Delta G = \nu_A \Delta\tilde{\mu}_A + (2f - 1)\nu_B \Delta\tilde{\mu}_B, \quad (3)$$

where the electrochemical gradient of species S is given by [15]

$$\Delta\tilde{\mu}_S = k_B T \ln\left(\frac{N_c^S/V_c}{N_p^S/V_p}\right) + Q_S \Delta\Psi, \quad (4)$$

k_B is the Boltzmann constant, T is temperature, and Q_S is the charge of a particle S. A $\Delta G < 0$ favors the influx of particles A, whereas a $\Delta G > 0$ favors the efflux of these particles. Thermodynamic equilibrium is reached when $\Delta G = 0$.

Our objective is to write a set of equations to describe the time evolution of this system. To do that, we need to obtain the 14 transition probabilities $W_{kk'}$, where the transition from k to k' is an allowed transition in the alternating access model (see Fig. 1). Each of these transition probabilities is a product of three components. The first component is $1/2$ for $k \in \{1, 3, 4, 6\}$; $\xi/3$ for W_{25} and W_{52}; and $\frac{1}{2}(1 - \xi/3)$ for W_{kk+1} and W_{kk-1} with $k \in \{2, 5\}$, where $\xi \in [0, 1]$. When $\xi = 0$, the conventional model is recovered, whereas $\xi = 1$ corresponds to the situation of maximum leakage. As one can see, we have assumed that, at each time step Δt, a cotransporter in state k can move forward to $k + 1$ or backward to $k - 1$ with equal probability amplitudes, as in the random-walk problem [16,17]. However, unlike this classic problem, the state transitions in a cotransport mechanism can be frustrated either by the concentration limitation, or by the Boltzmann factor, as described below.

The concentration limitation is associated with the second component of $W_{kk'}$, which is the probability of finding at least ν_S particles S close enough to be captured by a cotransporter in the C_{In} conformation, π_c^S, or in the C_{Out} conformation, π_p^S. Therefore, transitions that do not involve the binding of particles do not have this component. These probabilities can be calculated from statistical mechanics as [18,19]

$$\pi_\ell^S = \left(\frac{1}{C_0}\frac{N_\ell^S}{V_\ell}\right)^{\nu_S}, \quad (5)$$

where $\ell \in \{c, p\}$, and C_0 is a constant concentration whose value is of the order of $D^{-1}(r_A + r_B)^{-2}$, D being the largest dimension of the carrier protein along the membrane, and r_S the molecular radius of a S-type particle. In our model, for simplicity, we assume that the cotransporter will not capture particles one by one, but all at once. This assumption is reasonable when $N_\ell^S \gg \nu_S$, since under this condition, the time to capture all the particles is much smaller than the time to complete a whole cycle, which for LacY is approximately 56 ms [20]. Moreover this assumption significantly reduces the mathematical complexity of our model, since without it, the six-state cycle would become a $2(\nu_A + \nu_B + 1)$-state cycle.

The third component of $W_{kk'}$ is associated with the Boltzmann factor through the Metropolis acceptance probability, which is given by [21]

$$\alpha_{kk'} = \begin{cases} \exp(-\beta E_a), & E_a > 0 \\ 1, & E_a \leqslant 0 \end{cases}, \quad (6)$$

where E_a is the activation energy of the transition, and $\beta = 1/k_B T$. Intuitively, one can think of this component as an effective state transition probability once the events associated with the first two components of $W_{kk'}$ have occurred. In our

model it will be necessary to assume that E_a is equal to the free-energy variation $\Delta E_{kk'} = E_{k'} - E_k$, since it is usually not possible to obtain the activation energies for a given cotransporter, whereas a method to estimate its free-energy curve has already been established in the literature [2].

Next, we have to consider the contribution of $\Delta\Psi$ to the free-energy landscape of the transport cycle. To do this, we use the fact that, in both the C_{In} and C_{Out} conformations, the solvent-filled cavity of a cotransporter does not bear a significant part of the membrane electrostatic field [22], and hence the membrane potential can contribute only to transitions that involve a conformational change. Specifically, the terms

$$f\nu_A Q_A \Delta\Psi, \quad (\nu_A Q_A + f\nu_B Q_B)\Delta\Psi, \quad \text{and} \quad (f-1)\nu_B Q_B \Delta\Psi \tag{7}$$

have to be added, respectively, to the free-energy variations ΔE_{25}, ΔE_{34}, and ΔE_{61}. Furthermore, these terms have to be subtracted, respectively, from ΔE_{52}, ΔE_{43}, and ΔE_{16}. Thus, using Eqs. (6) and (7), the following relation between the Metropolis acceptance probabilities can be demonstrated:

$$\prod_k \frac{\alpha_{kk+1}}{\alpha_{k+1k}} = \exp\{-\beta[\nu_A Q_A + (2f-1)\nu_B Q_B]\Delta\Psi\}. \tag{8}$$

We are now ready to write the state transition probabilities based on the three components defined earlier and the alternating access model shown in Fig. 1. For instance, the transition probability W_{12} for a symporter is $\pi_p^A \alpha_{12}/2$, whereas that for an antiporter is $\alpha_{12}/2$. Therefore, it is straightforward to write the transition probability matrix

$$W = \begin{bmatrix} W_{11} & \gamma_p\alpha_{12} & 0 & 0 & 0 & \frac{1}{2}\alpha_{16} \\ \delta_p\alpha_{21} & W_{22} & \varepsilon_p\alpha_{23} & 0 & \frac{\xi}{3}\alpha_{25} & 0 \\ 0 & \frac{1}{2}\alpha_{32} & W_{33} & \frac{1}{2}\alpha_{34} & 0 & 0 \\ 0 & 0 & \frac{1}{2}\alpha_{43} & W_{44} & \frac{1}{2}\alpha_{45} & 0 \\ 0 & \frac{\xi}{3}\alpha_{52} & 0 & \varepsilon_c\alpha_{54} & W_{55} & \delta_c\alpha_{56} \\ \frac{1}{2}\alpha_{61} & 0 & 0 & 0 & \gamma_c\alpha_{65} & W_{66} \end{bmatrix}, \tag{9}$$

where $W_{kk} = 1 - \sum_{k'\neq k} W_{kk'}$ is the probability that a cotransporter in state k will not undergo any state transition, and we defined the parameters

$$\gamma_\ell = \frac{1}{2}(1 - f + f\pi_\ell^A),$$
$$\delta_\ell = \frac{1}{2}\left(1 - \frac{\xi}{3}\right)\left[f + (1-f)\pi_\ell^B\right],$$
$$\text{and} \quad \varepsilon_\ell = \frac{1}{2}\left(1 - \frac{\xi}{3}\right)\left[f\pi_\ell^B + (1-f)\pi_\ell^A\right]. \tag{10}$$

It is important to note that, although our model involves n cotransporters, the above matrix is the transition probability matrix between the six states of a single cotransporter.

As one can see, the model we are proposing is a random walk whose transition probabilities are time dependent and nonhomogeneous, that is, they depend on t and the states through π_ℓ^S and $\alpha_{kk'}$, respectively. To solve the random-walk problem, we will invoke the master equation (ME) approach [23]. Thus, to describe the time evolution of our system, we have six MEs for the variables $n_k(t)$,

$$\frac{dn_k}{dt} = \frac{1}{\Delta t}\sum_{k'\neq k}(W_{k'k}n_{k'} - W_{kk'}n_k), \tag{11}$$

and four MEs for the variables $N_\ell^S(t)$,

$$\frac{1}{\nu_S}\frac{dN_\ell^S}{dt} = \frac{h}{\Delta t}(W_{K+1K}n_{K+1} - W_{KK+1}n_K), \tag{12}$$

where h and K are, respectively, 1 and $2-f$ for N_p^A; $2f-1$ and $1+f$ for N_p^B; $1-2f$ and $5-f$ for N_c^B; and -1 and $4+f$ for N_c^A. These MEs form a set of 10 coupled differential equations that can be solved numerically using the finite difference method [24], where the derivative of a function $\varphi(t)$ is approximated by $\dot{\varphi} \approx [\varphi(t+\tau) - \varphi(t)]/\tau$. Our PYTHON code to solve this set of equations can be found in the Supplemental Material [25].

III. RESULTS AND DISCUSSIONS

First, we consider a case where no leakage is allowed, that is, $\xi = 0$. The objective is to validate our model by calculating the asymptotic behavior of the system. For this purpose, note that for $t \to \infty$ the derivatives on the left-hand side of Eqs. (11) and (12) vanish, leading to the following equilibrium relations:

$$n_1/n_6 = \alpha_{61}/\alpha_{16}, \quad n_3/n_4 = \alpha_{43}/\alpha_{34},$$
$$\text{and} \quad N_{\ell,\xi=0}^S = C_0 V_\ell \left(\frac{\alpha_{K+1K}}{\alpha_{KK+1}}\frac{n_{K+1}}{n_K}\right)^{h/\nu_S}. \tag{13}$$

These relations can be used together with Eq. (8) to show that

$$\frac{N_c^A/V_c}{N_p^A/V_p} = \left(\frac{N_p^B/V_p}{N_c^B/V_c}\right)^{(2f-1)\nu_B/\nu_A} \times \exp\left\{-\beta\left[Q_A + (2f-1)\frac{\nu_B}{\nu_A}Q_B\right]\Delta\Psi\right\}, \tag{14}$$

which is the static head equilibrium condition. The above equation is a well-known result for the cotransport that can also be obtained from thermodynamics by setting $\Delta G = 0$ in Eq. (3). Here we presented an independent derivation based on microscopic principles by mapping the alternating access model onto a random-walk model.

Now let us consider a system where $\xi \neq 0$. In this case, there is an additional equilibrium condition related to the leakage pathway between states 2 and 5,

$$n_2/n_5 = \alpha_{52}/\alpha_{25}. \tag{15}$$

Moreover, the asymptotic expression of $N_\ell^S(t)$ in Eq. (13) assumes the more general form

$$N_\ell^S = \left(1 - \frac{\xi}{3}\right)^{\tilde{h}/\nu_S} N_{\ell,\xi=0}^S, \tag{16}$$

where $\tilde{h}$ is $2f-1$ for N_ℓ^A and -1 for N_ℓ^B. Thus, using the result that summing the free-energy variations along a cycle in Fig. 1 is zero, it can be demonstrated that

$$\frac{N_c^S/V_c}{N_p^S/V_p} = \exp(-\beta Q_S \Delta\Psi), \tag{17}$$

which are two constraints valid for $\xi \neq 0$. Note that these constraints also lead to the static head equilibrium condition expressed in Eq. (14). In contrast, as we mentioned in the Introduction, some authors believe that any leakage is incompatible with the static head. Surprisingly, however, the above results demonstrate that our system converges to this equilibrium condition. Thus, one can conclude that the result in Eq. (14) is independent of the existence of a leak pathway across the cell membrane, although the final equilibrium configuration depends on the constraints in Eq. (17) when $\xi \neq 0$. Put more simply, the static head condition holds for any value of ξ, but for $\xi \neq 0$, these constraints reduce the number of degrees of freedom of the static head.

The above results appear to be in partial disagreement with the conclusion that, when leaks of either ligand are factored into the cotransport model, the only equilibrium that can exist is when the solutions on both sides of the transporter have equal ligand concentrations [11]. According to Eq. (17), we see that this conclusion is true only when the membrane potential $\Delta\Psi$ is zero and/or both species are electroneutral. Otherwise, the N_S particles S will tend to a distribution where the diffusion force due to the concentration gradient, $\Delta\mu_S$, compensates the electrical interaction of these particles with the cell membrane, and this distribution does not necessarily correspond to equal concentrations on both sides of the cotransporter. Importantly, we reinforce here that the final distribution of particles A and B is compatible with static head equilibrium under any conditions.

Next, we applied our model to the 1 : 1 symport catalyzed by LacY in which particles A and B correspond to H^+ and lactose, respectively. The free-energy variations of this symport were estimated from experimental data and are available in Fig. 1(b) of Ref. [2], as reproduced in the Supplemental Material [25]. Thus, using these free-energy variations and assuming that $\Delta\Psi = -100\,\mathrm{mV}$, which is a typical value for the membrane potential of *E. coli* [26], we calculated from Eq. (6) the 14 Metropolis acceptance probabilities for LacY. We performed simulations for ξ equal to 0 and 1.

The results for $\xi = 0$ are shown in Fig. 2. As one can see from this figure, the initial concentration of H^+ is higher in the periplasm than in the cytoplasm, and hence, according to Fick's law , there is a thermodynamic force pushing H^+ ions from the periplasm to the cytoplasm. In addition to this force, the membrane potential generates another force that also pushes H^+ ions from the periplasm to the cytoplasm. We thus expect $N_c^{H^+}$ to increase and $N_p^{H^+}$ to decrease until the equilibrium configuration is reached, in accord with the results in Fig. 2(a). On the other hand, Fig. 2(b) shows that there is a thermodynamic force pushing lactose molecules from the cytoplasm to the periplasm. However, what is observed is that the lactose molecules are being pumped against their concentration gradient, since N_c^L increases and N_p^L decreases. The energy to drive this lactose movement comes entirely from the downhill movement of H^+, and these two movements are coupled by LacY. In equilibrium, the system has approximately 25% of H^+ ions and 99% of lactose molecules in the cytoplasm. It can be verified that these values satisfy Eq. (14).

In Fig. 3 we present the results for the case of $\xi = 1$. From this figure, one can see that the time evolution of the system is completely different from that in Fig. 2, even though the

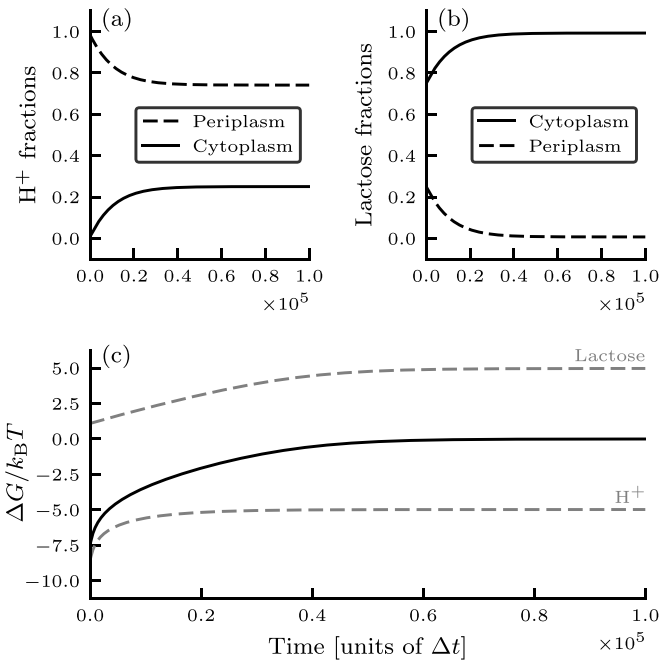

FIG. 2. Dynamics of lactose transport by LacY for $\xi = 0$. We used in all plots 10^6 time steps of $\tau = \Delta t/10$ for integrating Eqs. (11) and (12) with the following initial conditions: $n_1 = 10^3$, $n_{k\neq 1} = 0$, $N_p^{H^+} = 10^5$, $N_p^L = 2.5 \times 10^4$, $N_c^L = 7.5 \times 10^4$, $N_c^{H^+} = 10^3$. In addition, we considered that $V_c = V_p = 10^6/C_0$. (a) H^+ fractions in the cytoplasm and periplasm. (b) Lactose fractions in the cytoplasm and periplasm. (c) The variation in the Gibbs free-energy across the membrane is denoted by the solid black line. Also shown as dashed gray lines are the H^+ electrochemical gradient, $\Delta\tilde{\mu}_{H^+}$, and the lactose concentration gradient, $\Delta\mu_L$.

initial conditions are the same. First, a greater amount of H^+ ions was carried from the periplasm to the cytoplasm. Thus, by comparing Figs. 2(a) and 3(a), we can see that, in the second case, the H^+ ions were carried approximately four times faster than in the case of $\xi = 0$. This is due to the presence of an additional H^+ leakage pathway in our modified model. On the other hand, the lactose molecules took three times longer than the ions to reach their equilibrium state, whereas the final configuration of each species is reached simultaneously when $\xi = 0$. In fact, when we compare Figs. 2(b) and 3(b), we

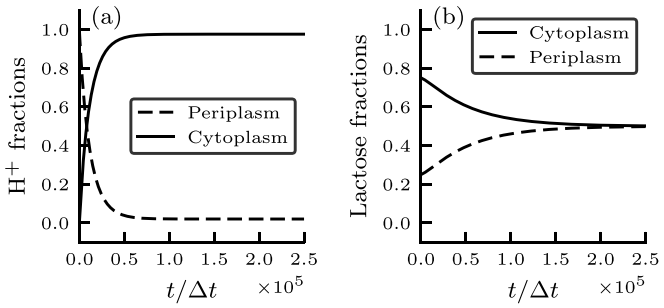

FIG. 3. Dynamics of lactose transport by LacY for $\xi = 1$. In all plots, we used 2.5×10^6 time steps of $\tau = \Delta t/10$ for integrating Eqs. (11) and (12) with the same initial conditions as in Fig. 2. (a) H^+ fractions in the cytoplasm and periplasm. (b) Lactose fractions in the cytoplasm and periplasm.

observe that the lactose molecules were moving 2.5 times slower in the second case than in the first case. Hence, the system as a whole has become slower when leakage is allowed. This result is counterintuitive, since without tightly coupling the movement of the driven and driving species, the system can operate as a symport and a uniport at the same time, and so LacY should work more efficiently. Instead, these two modes of operation are competing, and for the initial conditions of the system, the uniport of H^+ is being favored over the symport of lactose. In equilibrium, the system has approximately 98% of H^+ ions and 50% of lactose molecules in the cytoplasm. These values satisfy Eqs. (14) and (17).

To the best of our knowledge, the present model is the first to introduce the leak parameter ξ, and thus it is important to establish a way to estimate it. However, this is not a simple task, especially because we believe that this parameter is not a property of the cotransporter, and thus it can even depend on the initial conditions of the experiment. Moreover, the most accessible experimental quantities are the ratios between the equilibrium concentrations in Eq. (17), and these quantities do not depend on ξ. Nevertheless, there is a possible way to estimate this parameter if the ratio between the leak current,

$$I_{\text{leak}} = \frac{\xi \nu_A Q_A}{3\Delta t}(\alpha_{25} n_2 - \alpha_{52} n_5), \tag{18}$$

and the maximal cotransport current is known. For instance, as mentioned before, this ratio for the symport of Na^+ and glucose via the SGLT1 varies from 0.05 and 0.1, and thus the value of ξ could be adjusted in such a way that the ratio calculated by our model lies within the interval obtained experimentally. Unfortunately, for LacY, the value of this ratio is not known. This method for estimating ξ should be further investigated.

In summary, we presented a stochastic model based on the modified alternating access mechanism that correctly reproduced the cotransport dynamics found in the literature and is compatible with the static head equilibrium condition. This model can be used in the studies of cell mechanics, since ion pumps and cotransporters are essential for cells to maintain intracellular osmolyte concentrations, which in turn control cell pressure and volume. Thus, these ion channels and pumps should be considered in any cell mechanics simulation [27–29]. Our model can also be used to study the mechanosensitivity of cotransporters, which is a poorly studied problem on the interface between physics and biology with possible applications to heart disease therapies (for details, see Ref. [30]).

ACKNOWLEDGMENTS

This work was supported by Fundação de Amparo à Pesquisa do Estado de São Paulo (FAPESP), Grant No. 2019/16338-7, and Conselho Nacional de Desenvolvimento Científico e Tecnológico (CNPq), Processes No. 306849/2017-8 and No. CNPq_8844f602e8.

[1] L. R. Forrest, R. Krämer, and C. Ziegler, The structural basis of secondary active transport mechanisms, Biochim. Biophys. Acta-Bioenergetics **1807**, 167 (2011).

[2] Y. B. Barreto, M. L. Rodrigues, and A. M. Alencar, Transport cycle of *Escherichia coli* lactose permease in a nonhomogeneous random walk model, Phys. Rev. E **99**, 052411 (2019).

[3] L. Guan and H. R. Kaback, Lessons from lactose permease, Annu. Rev. Biophys. Biomol. Struct. **35**, 67 (2006).

[4] M. P.Blaustein and W. J. Lederer, Sodium/calcium exchange: Its physiological implications, Physiol. Rev. **79**, 763 (1999).

[5] O. Jardetzky, Simple allosteric model for membrane pumps, Nature (London) **211**, 969 (1966).

[6] J. Abramson, I. Smirnova, V. Kasho, G. Verner, H. R. Kaback, and S. Iwata, Structure and mechanism of the lactose permease of *Escherichia coli*, Science **301**, 610 (2003).

[7] O. Andrini, C. Ghezzi, H. Murer, and I. C. Forster, The leak mode of type II Na^+-Pi cotransporters, Channels **2**, 346 (2008).

[8] W. Stein, *Transport and Diffusion across Cell Membranes* (Elsevier Science, Orlando, Florida, 2012).

[9] J.-P. Longpré, D. G. Gagnon, M. J. Coady, and J.-Y. Lapointe, The actual ionic nature of the leak current through the Na^+/glucose cotransporter SGLT1, Biophys. J. **98**, 231 (2010).

[10] J. J. Centelles, R. K. H. Kinne, and E. Heinz, Energetic coupling of Na-glucose cotransport, Biochim. Biophys. Acta-Biomembranes **1065**, 239 (1991).

[11] R. J. Naftalin, Reassessment of models of facilitated transport and cotransport, J. Membr. Biol. **234**, 75 (2010).

[12] E. K. Cloherty, K. S. Heard, and A. Carruthers, Human erythrocyte sugar transport is incompatible with available carrier models, Biochemistry **35**, 10411 (1996).

[13] R. J. Naftalin, The thermostatics and thermodynamics of cotransport, Biochim. Biophys.-Biomembranes **778**, 155 (1984).

[14] D. Walz and S. R. Caplan, The thermostatics and thermodynamics of cotransport revisited: A restatement of the zeroth law, Biochim. Biophys. Acta-Biomembranes **859**, 151 (1986).

[15] D. L. Nelson, A. L. Lehninger, and M. M. Cox, *Lehninger Principles of Biochemistry* (Macmillan, New York, 2008).

[16] F. Spitzer, *Principles of Random Walk*, Graduate Texts in Mathematics Vol. 34 (Springer Science & Business Media, New York, 2013).

[17] M. Menshikov, S. Popov, and A. Wade, *Non-homogeneous Random Walks: Lyapunov Function Methods for Near-Critical Stochastic Systems*, Cambridge Tracts in Mathematics Vol. 209 (Cambridge University Press, Cambridge, 2016).

[18] A. M. Alencar, J. P. Butler, and S. M. Mijailovich, Thermodynamic origin of cooperativity in actomyosin interactions: The coupling of short-range interactions with actin bending stiffness in an Ising-like model, Phys. Rev. E **79**, 041906 (2009).

[19] R. Phillips, J. Kondev, J. Theriot, and H. Garcia, *Physical Biology of the Cell* (CRC Press, Boca Raton, FL, 2012).

[20] I. Smirnova, V. Kasho, J. Sugihara, and H. R. Kaback, Opening the periplasmic cavity in lactose permease is the limiting step for sugar binding, Proc. Natl. Acad. Sci. USA **108**, 15147 (2011).

[21] K. Binder and D. W. Heermann, *Monte Carlo Simulation in Statistical Physics: An Introduction*, Graduate Texts in Physics (Springer, Berlin, 2010).

[22] X. C. Zhang, Y. Zhao, J. Heng, and D. Jiang, Energy coupling mechanisms of MFS transporters, Protein Sci. **24**, 1560 (2015).

[23] V. M. Kenkre, E. W. Montroll, and M. F. Shlesinger, Generalized master equations for continuous-time random walks, J. Stat. Phys. **9**, 45 (1973).

[24] T. J. R. Hughes, *The Finite Element Method: Linear Static and Dynamic Finite Element Analysis* (Courier Corporation, Mineola, New York, 2012).

[25] See Supplemental Material at http://link.aps.org/supplemental/10.1103/PhysRevE.102.022403 for the PYTHON code used to solve the set of master equations.

[26] H. Felle, J. S. Porter, C. L. Slayman, and H. R. Kaback, Quantitative measurements of membrane potential in *Escherichia coli*, Biochemistry **19**, 3585 (1980).

[27] A. M. Alencar, M. S. A. Ferraz, C. Y. Park, E. Millet, X. Trepat, J. J. Fredberg, and J. P. Butler, Non-equilibrium cytoquake dynamics in cytoskeletal remodeling and stabilization, Soft Matter **12**, 8506 (2016).

[28] J. Tao, Y. Li, D. K. Vig, and S. X. Sun, Cell mechanics: A dialogue, Rep. Prog. Phys. **80**, 036601 (2017).

[29] C. Y. Park, D. Tambe, A. M. Alencar, X. Trepat, E. H. Zhou, E. Millet, J. P. Butler, and J. J. Fredberg, Mapping the cytoskeletal prestress, Am. J. Physiol.-Cell Physiol. **298**, C1245 (2010).

[30] V. S. Markin and F. Sachs, Thermodynamics of mechanosensitivity, Phys. Biol. **1**, 110 (2004).